PROTOTYPE PICK-UP TANK FOR CR STOCHASTIC COOLING AT FAIR*

F. Nolden, R. Hettrich, U. Jandewerth, C. Peschke, P. Petri, M. Steck, GSI, Darmstadt, Germany

Abstract

A prototype pick-up tank for stochastic precooling in the CR storage ring of the FAIR project at GSI was built. It will be equipped with movable electrodes driven by linear motors. The electrodes can be operated at cryogenic temperatures. The design of the tank and first test measurements are presented.

INTRODUCTION

The Collector Ring CR [1, 2] is a storage ring within the FAIR project at GSI which has three purposes: stochastic cooling of radioactive ion beams, stochastic cooling of antiproton beams, and nuclear mass measurements of short-lived nuclei in an isochronous optical setting. These beams are injected at high emittances and momentum spreads immediately after production. They have a short bunch length of about 50 ns; their momentum spread is therefore reduced by bunch rotation and subsequent adiabatic debunching. Two different optical settings are required for ions and antiprotons. Due to their different energies, the frequency slip factors must be different in order to achieve optimum conditions for stochastic cooling.

Table 1: Basic Parameters of the CR

	rare isotopes	antiprotons
circumference	216.25 m	
max. magnetic rigidity	13 Tm	
energy	740 MeV/u	3.0 GeV
Lorentz β	0.83	0.97
Lorentz γ	1.80	4.20
max. number of particles	$1 \cdot 10^9$	$1 \cdot 10^8$
charge state	up to 92	-1

The beam parameters after adiabatic debunching and at the end of the cooling process are listed in Table 1. Three pick-up tanks and three kicker tanks will be installed at locations of zero dispersion in the long straight sections. A further pick-up tank is needed for Palmer cooling of radioactive beams, which is located in an arc at high dispersion.

Here we discuss the prototype design of a pick-up tank at zero dispersion. The design is made such that it could serve as either a horizontal pick-up or, after rotation by 90 degrees, as a vertical pick-up.

Table 2 displays the initial and final beam parameters for rare isotope and antiproton beams. In order to reach the required final emittances, a good signal-to noise ratio is indispensable. Therefore a tank design with movable (plunging) electrodes was adopted.

Table 2: Initial and Final Beam Parameters for CR

	rare isotopes	
	$\delta p/p$ (2σ)	ϵ_{xy} [mm mrad]
injected	1.5 %	200
debunched	0.4 %	200
cooled	0.05 %	0.5
total cooling time [s]	1.5	
	antiprotons	
	$\delta p/p$ (2σ)	ϵ_{xy} [mm mrad]
injected	3.0 %	240
debunched	0.7 %	240
cooled	0.1 %	5
total cooling time [s]	10	

The layout of the straight sections in the CR follows a FODO design [3]. Along the length of the 2m long pick-up tank, the slope of the betatron function is non-negligible, and the beam envelopes change substantially. Table 3 lists the vertical radius inside the pick-ups P1 and P2 in the beginning and at the end of cooling, both at the entrance and the exit of the tank. Table 4 shows the analogous data for the tank P3, where the electrodes are arranged horizontally. The signal from these tanks is produced by electrodes arranged above and below the beam (vertical pick-up). In the course of the cooling process the beam size decreases substantially, in particular for the radioactive beams.

Table 3: Vertical Beam Radius (in mm) for Pick-ups P1 and P2

	P1			
	initial		final	
	entrance	exit	entrance	exit
pbar	56	41	8	6
RIB	58	49	3	3
	P2			
	initial		final	
	entrance	exit	entrance	exit
pbar	37	43	6	6
RIB	42	52	2	3

Table 4: Horizontal Beam Radius (in mm) for Pick-up P3

	initial		final	
	entrance	exit	entrance	exit
pbar	52	40	7	6
RIB	57	47	3	2

* Work supported by EU design study (contract 515873 - DIRAC-secondary-Beams)

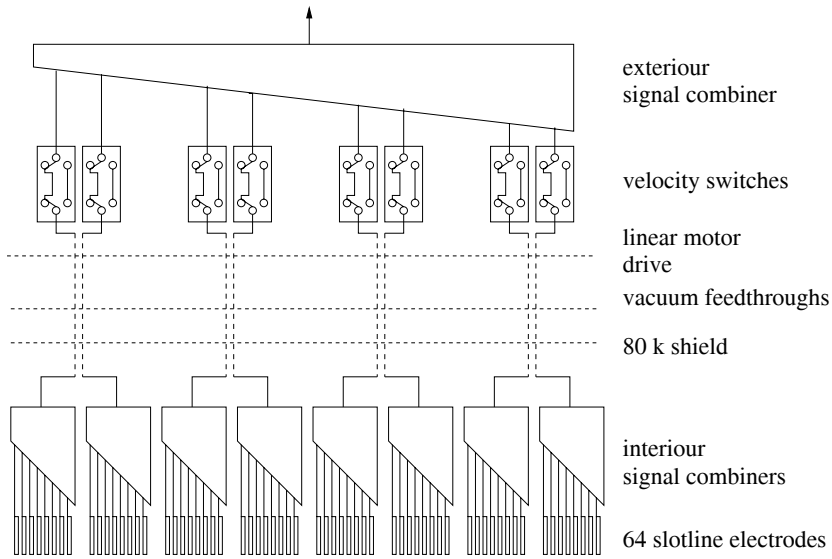

Figure 1: Sketch of signal paths in pick-up.

TANK ARCHITECTURE

The signals arise from slotline electrodes. Their design has been developed in the past years through a series of optimization procedures [4]. Eight of these electrodes are arranged on a single pcb (printed circuit bord). Because the beam velocities of radioactive ions and antiprotons are different, one has to pay attention to the phase-correct combination of the signals from each electrode. Because of their low charge state, the signal to noise ratio is most critical for antiprotons. We assume in the following that each slotline delivers a voltage U_0. The signal combiner is optimized with respect to to the velocity β_1 of the antiprotons. If the beam velocity β_2 is different from this velocity, and if one uses n_p pick-up electrodes arranged at a distance d_p, then one gets from an ideal power combiner a sum voltage

$$\begin{aligned} U &= \frac{U_0}{\sqrt{n_p}} \sum_{n=0}^{n_p-1} e^{-i\omega t_m} \qquad (1) \\ &= \frac{U_0}{\sqrt{n_p}} \frac{\sin\left(n_p \omega t_m/2\right)}{\sin\left(\omega t_m/2\right)} e^{-i(n_p-1)\omega t_m/2} \end{aligned}$$

with the mismatching time between electrodes

$$t_m = \frac{d_p}{c}\left(\frac{1}{\beta_1} - \frac{1}{\beta_2}\right) \qquad (2)$$

Taking the signal from eight electrodes in a row with a distance d_p of 25 mm between electrodes, the phase error for radioactive ions leads to an acceptable maximum combination loss of 0.8 dB at the upper band limit of 2 GHz. The electrode pcb is mounted to the front side of an aluminum body. Inside this body eight chambers exist, inside which the signal is transported to the rear side. Here the signal from eight electrodes is power combined. Then the signal is transported by coaxial lines attached to a solid carrier rod towards the outside of the tank. Each carrier rod transports the signal of two neighbouring eight-slot pcbs. This mechanism is mechanically movable with a maximum amplitude of 60 mm. There are four movable mechanical systems on each side of the tank. The aluminum body inside the tank is cooled to a temperature of 20 K. The thermal contact between the helium cold heads and the aluminum body is maintained by movable silver-coated copper-beryllium sheets.

These cold parts are shielded from the room temperature surroundings by means of a gilded copper cylinder which is kept at a temperature of 80 K. The gold surface is 4 μm thick and has an extremely low thermal emissivity. Between the copper body and the gold surface there is a thin intermediate nickel layer which prevents diffusion of copper into the gold.

After passing coaxial ceramic feedthroughs, the signal is fed into high quality movable cables outside the vacuum tank. Here the signal will be amplified by cryogenic low-noise preamplifiers at a temperature of 80 K. Between these cables and the final eight-fold combiner, switches are mounted which add a proper delay to the radioactive beam signal, if needed.

JERK FREE MOVEMENT PROFILES

For the linear drives a maximum movable path of 60 mm is foreseen. The fastest movement occurs when the device is driven in order to admit a fresh injection of secondary radioactive beams. In this case a distance of $S = 60$ mm must be covered within a time interval $T = 200$ ms.

Such movements have a typical path scale S, a typical time scale T, a typical velocity scale $V = S/T$, and a typical acceleration scale $A = S/T^2$. The velocity vanishes at the beginning and at the end of the movement. One can easily see that such a movement requires at least an acceleration of $4A$. To avoid excitation of mechanical resonances

inside the structure the acceleration profile $a(t)$ should be as smooth as possible, because the mechanical excitations are expected to be caused by the Fourier components $a(\omega)$ of the acceleration profile at the mechanical resonances ω. For such jerk-free profiles one requires in addition that the acceleration must vanish in the beginning and at the end of the motion, as well. A well-known example of such a profile is the fifth order polynomial

$$s(t) = S\left[\frac{1}{2} + \frac{1}{16}\left(15\tau - 10\tau^3 + 3\tau^5\right)\right] \tag{3}$$

with the normalized time variable

$$\tau = \frac{2t}{T} - 1, \quad -1 \le \tau \le 1 \tag{4}$$

Several movement profiles were investigated theoretically. As long as the resonances are unknown, the following criteria can be useful for optimized profiles:

1. The accelerating 'energy' $E_{\mathrm{acc}} = \int |a(t)|^2 dt$ of the movement should be minimized. By Parseval's theorem, this quantity can be expressed by the Fourier transform $a(\omega)$, as well: $E_{\mathrm{acc}} = (2\pi)^{-1} \int |a(\omega)|^2 dt$.

2. The maximum acceleration $a_{\max}$ should be minimized.

3. The excitation frequency $a(\omega)$ should decay rapidly towards high frequency.

It turned out that harmonic profiles of the form

$$s(t) = S\left[\frac{1}{2} + \frac{1}{2}\tau + \sum_{n=0}^{N} b_n \sin\left((2n+1)\pi\tau\right)\right] \tag{5}$$

$$a(t) = -4A\pi^2 \sum_{n=0}^{N} b_n \left(2n+1\right)^2 \sin\left((2n+1)\pi\tau\right) \tag{6}$$

have very convenient properties. Their acceleration spectrum decreases much faster at high harmonics than profiles using polynomial approaches, such as the 5th order polynomial. Their 'energy' E_{acc} values as well as their minimum accelerations are also rather small.

The Fourier transform of the acceleration profile must be calculated using the condition that it vanishes outside the time interval $\tau \in \{-1, +1\}$. This is taken into account by multiplication with a function $p_1(\tau)$ which is equal to one in this interval and vanishes outside:

$$\begin{aligned} & \mathcal{F}\left\{\sin((2n+1)\pi\tau)\, p_1(\tau)\right\} \\ = & \int_{-1}^{1} \sin\left((2n+1)\pi\tau\right) e^{-i\omega\tau} d\tau \\ = & \frac{1}{i}\left[\frac{\sin\left((2n+1)\pi - \omega\right)}{(2n+1)\pi - \omega} - \frac{\sin\left((2n+1)\pi + \omega\right)}{(2n+1)\pi + \omega}\right] \\ = & \frac{\sin\omega}{i} \frac{2(2n+1)\pi}{\left((2n+1)\pi\right)^2 - \omega^2} \end{aligned} \tag{7}$$

These spectra decrease proportionally to ω^{-2} for large frequencies, therefore the spectral energy of the acceleration is well concentrated around frequencies $f = \omega/2\pi = 1/T$. In contrast the spectra of polynomial-type profiles decay proportionally to ω^{-1} only. This can be derived from the recursion relations ($\omega \neq 0$)

$$\begin{aligned} & \mathcal{F}\left\{\tau^n p_1(t)\right\} = \int_{-1}^{1} \tau^n e^{-i\omega\tau} d\tau \\ = & \frac{-1}{i\omega}\tau^n e^{-i\omega\tau}\Big|_{-1}^{1} + \frac{n}{i\omega}\int_{-1}^{1} \tau^{n-1} e^{-i\omega\tau} d\tau \\ = & \begin{cases} \frac{2\sin\omega}{\omega} + \frac{n}{i\omega}\mathcal{F}\left\{\tau^{n-1} p_1(t)\right\} & n \text{ even} \\ \frac{2i\cos\omega}{\omega} + \frac{n}{i\omega}\mathcal{F}\left\{\tau^{n-1} p_1(t)\right\} & n \text{ odd} \end{cases} \end{aligned} \tag{8}$$

Table 5: Harmonic Coefficients

	b_0	b_1
sinusoidal profile ($N = 0$)	0.15915	-
$N = 1$, minimum $a_{\max}$	0.14957	0.003195
$N = 1$, minimum E_{acc}	0.14324	0.005305

Table 5 shows the coefficients of a purely sinusoidal profile, and of two profiles with a higher harmonic, namely the one with minimized maximum acceleration, and the one with minimum 'energy'. It is obvious that one gets a substantialy lower maximum acceleration and also a lower 'energy' by adding a small third harmonic to the path profile.

Table 6: Maximum Velocity, Acceleration and Energy of Harmonic Profiles

	$\frac{v_{\max}}{V}$	$\frac{a_{\max}}{A}$	$\frac{E_{\mathrm{acc}}}{A^2 T}$
sinusoidal profile ($N = 0$)	2.00	6.28	19.74
$N = 1$,minimum $a_{\max}$	2.00	5.13	18.08
$N = 1$, minimum E_{acc}	2.00	5.32	17.77

LINEAR MOTOR DRIVES

The linear drives (see fig. 3) use a Bobolowski DTL 85/205 motor. The primary and secondary parts of this motor are not coupled mechanically. The absence of friction inside the linear motor promises to be a good condition for long lifetime. The motor can deliver a maximum force of 280 N along a maximum length of 85 mm. Compression springs help accelerating the movable parts when the device is to be moved outside.

Different forces act on the drive:

- inertial forces due to the acceleration of the 25 kg support structure with rod and aluminum body,

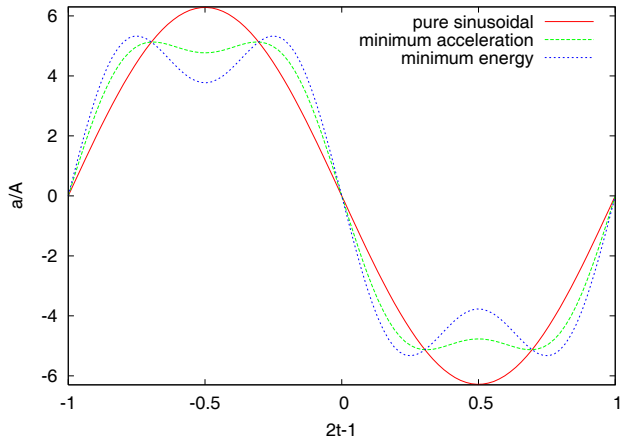

Figure 2: Harmonic acceleration profiles.

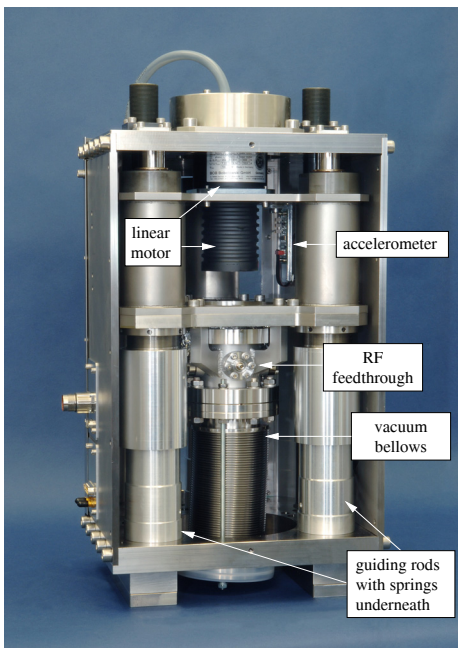

Figure 3: Linear drive before installation.

- the vacuum pressure of about 420 N,
- the force of the compression springs (about 100N),
- spring-like forces of the vacuum bellows,
- friction forces,
- gravitational forces in case of vertical mounting.

The springs are dimensioned such that they move the device to an outer stand-by position in case of a motor failure. The motor can keep the electrodes close to the beam (e.g. 10 mm) at the end of a cooling cycle. The fast outward directed movement is performed by the motor with effective assistance from the compression springs.

Each linear motor is controlled by a motor controller. The currents delivered to the motor depend on digital settings of the PI control parameters. If these are set correctly, a smooth motion of the motor can be established. The device is equipped with an optical position measurement system informing the controller at a rate of about 20 ks with a precision of less than ten μm. The controllers of the 8 different drives are synchronized via an ethercat bus system.

Figure 3 shows a photograph of the motor drive unit. The springs are mounted on each of three guiding rods providing the alignment of the primary and secondary parts of the motor. In order to detect unwanted vibrations an accelerometer is installed, which is sensitive in all three space directions. Its signals can interlock the motor controller as soon as their amplitude exceeds a predefined threshold.

MECHANICAL TANK DESIGN

The prototype vacuum tank has a length of 2.2 m and an inner diameter of 450 mm. A photography is shown in Fig. 4. The tank has four flanges for the linear drives on each side. There are two large flanges for Helium cold heads. In order to mount equipment inside, the tank has eight large flanges on each side, which are opened only for assembly or disassembly of electrodes, cables etc.

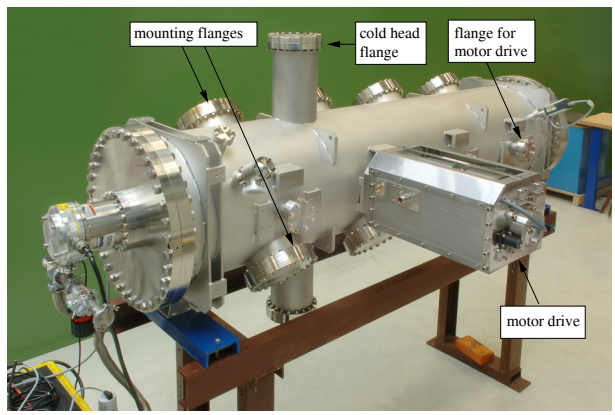

Figure 4: Tank prototype.

The vacuum vessel was delivered by end of 2008, two linear drives were installed by spring 2009. At present we are performing various movement studies. Both drives can be run simultaneously.

REFERENCES

[1] F. Nolden et al., "Stochastic Cooling Developments at GSI", *AIP Conference Proceedings*, **821** (2005), 177-184.

[2] F. Nolden, et al., "The Collector Ring CR of the FAIR Project", MOPCH077, *Proc. EPAC'06* (2006) 208-210

[3] A. Dolinskii, F. Nolden, M. Steck, "Lattice Considerations for the Collector and the Accumulator Ring of the FAIR Project", TUA2C08, *Proc. Cool 200*), 106-109

[4] C. Peschke, U. Jandewerth, F. Nolden, P. Petri, M. Steck, "Prototype Pick-up Module for CR Stochastic Cooling at FAIR", THPMCP003, *Proc. Cool 2009* (2009)